2010

Topological multicritical point in the phase diagram of the toric code model and three-dimensional lattice gauge Higgs model

I Tupitsyn

A Kitaev

Nikolai Prokof'ev
University of Massachusetts - Amherst, prokofev@physics.umass.edu

P.C.E Stamp

Topological multicritical point in the Toric Code and 3D gauge Higgs Models

I.S. Tupitsyn,[1] A. Kitaev,[2] N.V. Prokof'ev,[3] and P.C.E. Stamp[1]

[1] *Pacific Institute of Theoretical Physics, University of British Columbia, 6224 Agricultural Road, Vancouver, BC V6T 1Z1, Canada*

[2] *California Institute of Technology, Pasadena, California 91125, USA*

[3] *Department of Physics, University of Massachusetts, Amherst, Massachusetts 01003, USA*

(Dated: April 20, 2008)

We report a new type of multicritical point that arises from competition between the Higgs and confinement transitions in a $\mathbb{Z}_2$ gauge system. The phase diagram of the 3d gauge Higgs model has been obtained by Monte-Carlo simulation on large (up to 60^3) lattices. We find the transition lines continue as 2nd-order until merging into a 1st-order line. These findings pose the question of an effective field theory for a multicritical point involving noncommuting order parameters. A similar phase diagram is predicted for the 2-dimensional quantum toric code model with two external fields, h_z and h_x; this problem can be mapped onto an anisotropic 3D gauge Higgs model.

PACS numbers:

Introduction. Topological quantum phases and anyons are well known in connection with the fractional quantum Hall effect, but they are also expected to exist in frustrated magnets. It has long been proposed that a certain class of resonating-valence-bond (RVB) [1] phases carries $\mathbb{Z}_2$-charges and vortices and has a four-fold degenerate ground state on a torus [2]. A qualitative understanding of this phase can be obtained from a so-called *toric code model* (TCM) [3]. The dimer model on the Kagome lattice is mapped onto the TCM exactly [4] while some other models [5, 6] belong to the same universality class.

The TCM is defined in terms of spin-1/2 degrees of freedom located on the bonds of an arbitrary $2d$ lattice. The Hamiltonian is as follows:

$$H_{TC} = -J_x \sum_s A_s - J_z \sum_p B_p, \qquad (1)$$

where $A_s = \prod_{j\in s} \sigma_j^x$ and $B_p = \prod_{j\in p} \sigma_j^z$ are products of spin operators (σ_j^α are the Pauli matrixes) on the bonds incident to a lattice site s and on the boundary of a plaquette p, respectively. The ground state corresponds to eigenvalues $A_s = 1$, $B_p = 1$ for all s and p. On a surface of genus g, it is 4^g-fold degenerate. Elementary excitations are characterized by eigenvalues $A_s = -1$ (a $\mathbb{Z}_2$ charge on site s) and $B_p = -1$ (a $\mathbb{Z}_2$ vortex on plaquette p); all excitations are gapped. Each type of quasiparticle is bosonic, but due to nontrivial mutual braiding, they must be jointly regarded as *Abelian anyons*.

The Hamiltonian (1) has special properties related to its exact solvability: the two-point correlator vanishes and the quasiparticles have flat dispersion. These features do not survive a small generic perturbation, while the topological character of the ground state and the anyonic quasiparticle statistics are robust. Yet a sufficiently strong field can polarize the spins, driving a transition to the topologically trivial phase. Trebst *at al* [7] studied a perturbation of the form $-h\sum_b \sigma_b^z$ and solved the problem by reducing it to the $2d$ transverse-field Ising model, which is mapped to an anisotropic $3d$ classical Ising model. In this paper we consider a more general Hamiltonian:

$$H_Q = H_{TC} - h_x \sum_b \sigma_b^x - h_z \sum_b \sigma_b^z, \qquad (2)$$

where b runs over the bonds of a square lattice and H_{TC} is given by Eq. (1). Note that the fields h_x and h_z induce different types of phase transition. The term with h_z creates virtual pairs of $\mathbb{Z}_2$ charges, which condense when the field strength exceeds a certain threshold. This phenomenon may be described as a Higgs transition, or as vortex confinement. By duality, the field h_x causes the condensation of vortices and charge confinement. The competition of the two terms should result in an interesting phase diagram, which is the subject of this paper.

We approach the problem by reducing the quantum Hamiltonian to a classical *anisotropic* $\mathbb{Z}_2$ gauge Higgs Hamiltonian on a three-dimensional cubic lattice; see Eq. (5) below. We expect the phase diagram to be qualitatively similar to that for the *isotropic case*, i.e., model $M_{3,2}$ as defined by Wegner [8]. Monte-Carlo simulations have been performed for the latter model because it is more amenable to numerics. Some properties of the phase diagram in the isotropic case were predicted by Fradkin and Shenker [9]. In particular, the topological phase is bounded by second-order lines corresponding to charge condensation (for $h_x \ll h_z \sim J_x, J_z$) and vortex condensation (for $h_z \ll h_x \sim J_x, J_z$), but the two condensate phases are continuously connected. For the quantum Hamiltonian (2), a connecting path is realized by increasing h_z so as to polarize the spins in the z direction, rotating the field in the xz-plane, and decreasing it again. However, the two phase transitions are clearly different, therefore the corresponding lines cannot join smoothly.

A previous numerical study involving 10^3 sites by Jongeward, Stack, and Jayaprakash [10] showed the two

lines merge into a first-order line that partially separates the charge and vortex condensates, and suggested the 2nd-order lines might become 1st-order before merging. As discussed below, our data for larger systems (up to 60^3 sites) do not confirm this conjecture. Thus, the point where all three lines meet is likely to be a novel type of multicritical point. Note that each of the 2nd-order transitions can be characterized by an Ising-type order parameter, i.e., the amplitude of the corresponding condensate. The two parameters must somehow coexist though they are incompatible at the classical level due to the nontrivial braiding between charges and vortices. (ie., the kinetic terms describing the charge and vortex transport do not commute.)

The reduction to a classical problem. The Hamiltonian (2) is not gauge-invariant, but it can be mapped to a $\mathbb{Z}_2$ gauge theory by introducing a dummy spin variable μ_s ("matter field") at every site, but only considering states $|\Psi\rangle$ such that $\mu_s^x|\Psi\rangle = |\Psi\rangle$. This constraint is a prototype of the gauge-invariance condition, $\mu_s^x A_s|\Psi\rangle = |\Psi\rangle$, which says that flipping the spin on a site and all incident bonds does not change the state. To turn one constraint into the other, we apply the transformation:

$$\begin{aligned} \sigma_{uv}^z &\to \mu_u^z \sigma_{uv}^z \mu_v^z, \qquad & \sigma_{uv}^x &\to \sigma_{uv}^x, \\ \mu_s^z &\to \mu_s^z, & \mu_s^x &\to \mu_s^x A_s, \end{aligned} \tag{3}$$

where σ_{uv} belongs to the bond connecting sites u and v. Then, the Hamiltonian becomes:

$$H = -J_x \sum_s \mu_s^x - J_z \sum_p B_p - h_x \sum_b \sigma_b^x - h_z \sum_{uv} \mu_u^z \sigma_{uv}^z \mu_v^z. \tag{4}$$

Note that in the first term we have replaced A_s by μ_s using the gauge-invariance condition, $\mu_s^x A_s \equiv 1$.

We now map this 2-d quantum Hamiltonian onto a (2+1)-d classical one. The overall scheme is standard [11], but some care should be taken to preserve the gauge invariance. We let $\Delta\tau = \beta/n$, and approximate the quantum partition function $Z = \mathrm{Tr}[\exp(-\beta H)\mathcal{P}]$ by $\mathrm{Tr}[\exp(-\Delta\tau\, H_x)\mathcal{P}\exp(-\Delta\tau\, H_z)]^n$, where $\mathcal{P}$ is the projector onto the gauge-invariant subspace and H_x, H_z are the terms in the quantum Hamiltonian that depend on σ_b^x, μ_s^x and σ_b^z, μ_s^z, respectively. This expression can be written as a classical partition function on a cubic lattice. The classical variables $\sigma_{b,t}, \mu_{s,t} = \pm 1$, in each time slice t, correspond to σ_b^z and μ_s^z respectively. But when we change from $2d$ to $3d$, new vertical bonds (along the time direction) appear. The classical spins on the vertical bonds between two time slices correspond to a choice of term in the expansion of $\mathcal{P} = \prod_s \left(\frac{1}{2}(1 + \mu_s^x A_s)\right)$. Thus we arrive at this classical Hamiltonian:

$$H_C = -\sum_{uv} \lambda_{\mathrm{bond}}^{||,\perp} \mu_u \sigma_{uv} \mu_v - \sum_{\mathrm{p}} \lambda_{\mathrm{pl}}^{||,\perp} \prod_{j\in \mathrm{p}} \sigma_j; \tag{5}$$

$$\lambda_{\mathrm{bond}}^{||} = -\frac{1}{2}\ln\tanh \tilde{J}_x \quad - \text{vertical bonds;} \tag{6a}$$

$$\lambda_{\mathrm{bond}}^{\perp} = \tilde{h}_z \quad - \text{horizontal bonds;} \tag{6b}$$

$$\lambda_{\mathrm{pl}}^{||} = -\frac{1}{2}\ln\tanh \tilde{h}_x \quad - \text{vertical plaquettes;} \tag{6c}$$

$$\lambda_{\mathrm{pl}}^{\perp} = \tilde{J}_z \quad - \text{horizontal plaquettes,} \tag{6d}$$

where $\tilde{J}_x = J_x\Delta\tau$, $\tilde{J}_z = J_z\Delta\tau$, $\tilde{h}_x = h_x\Delta\tau$, $\tilde{h}_z = h_z\Delta\tau$. This model is an anisotropic generalization of the $\mathbb{Z}_2$ gauge Higgs model [9].

As a final step, we eliminate the redundancy by fixing μ_s. This only changes the classical partition function by a constant factor since Hamiltonian (5) can be written in terms of the gauge-invariant variables $S_{uv} = \mu_u \sigma_{uv} \mu_v$:

$$\widetilde{H}_C = -\sum_b \lambda_{\mathrm{bond}}^{||,\perp} S_b - \sum_{\mathrm{p}} \lambda_{\mathrm{pl}}^{||,\perp} \prod_{j\in \mathrm{p}} S_j. \tag{7}$$

More detailed calculations show that the quantum and classical partition functions are related by

$$Z = \left(\tfrac{1}{2}\sinh(2\tilde{J}_x)\right)^{k/2} \left(\tfrac{1}{2}\sinh(2\tilde{h}_x)\right)^{m/2} \widetilde{Z}_C, \tag{8}$$

where k and m are the number of vertical bonds and plaquettes, respectively.

Of course, Eq. (8) holds only in the limit $\Delta\tau \to 0$. However, we take the liberty of parametrizing the general classical Hamiltonian (7) by $\tilde{J}_x$, $\tilde{J}_z$, $\tilde{h}_x$, $\tilde{h}_z$, even though the corresponding quantum problem may not be defined. In the isotropic case, two parameters will suffice:

$$\widetilde{H}_C = -\lambda_{\mathrm{bond}} \sum_b S_b - \lambda_{\mathrm{pl}} \sum_{\mathrm{p}} \prod_{j\in \mathrm{p}} S_j, \tag{9}$$

where $\lambda_{\mathrm{bond}} = \tilde{h}_z$, $\lambda_{\mathrm{pl}} = -\frac{1}{2}\ln\tanh\tilde{h}_x$. This model is equivalent to the isotropic $\mathbb{Z}_2$ gauge Higgs model [9] and in what follows we compute its phase diagram.

Phase diagram in the isotropic case. At $\lambda_{\mathrm{bond}} = 0$ all configurations, including ground states, have the same degeneracy factor 2^{2N}. The actual physical variables in this limit are plaquette numbers $N_p = \prod_{j\in \mathrm{p}} S_j$, and the model itself is *dual* to the 3D classical Ising model (Eq. (9) is also known as the 3D Ising gauge theory [8]). Using high-accuracy results of Ref. [12] for the critical point and the duality relation $\lambda_{\mathrm{pl}} = -1/2\ln\tanh(J/T)$, where J is the Ising exchange coupling, we obtain $\lambda_{\mathrm{pl}}^{(c)} = 0.7614125$.

At arbitrary values of λ_{bond} and λ_{pl} the model is *self-dual* [13], i.e. it maps to itself under the coupling constant transformation $\lambda_{\mathrm{bond,pl}} \to -1/2\ln\tanh(\lambda_{\mathrm{pl,bond}})$. This means that the phase diagram has a symmetry, or *self-duality*, line defined by $\lambda_{\mathrm{bond}} = -1/2\ln\tanh(\lambda_{\mathrm{pl}})$. Under the duality mapping $(\lambda_{\mathrm{bond}} = 0, \lambda_{\mathrm{pl}} = 0.7614125) \to (\lambda_{\mathrm{bond}} = 0.221655, \lambda_{\mathrm{pl}} = \infty)$, which gives us two Ising-type critical points on the phase diagram.

To calculate the rest of the phase diagram we performed Monte Carlo simulations using standard single-spin flip updates, supplemented by rare (once per N^2 updates) flips of all spins belonging to bonds cut by planes oriented along any one of the crystal axes, or along any of the diagonals to these axes. There are $9N$ possible planes satisfying this condition, and we select any of them at random. The plaquette energy (second term in (9)) is conserved by this update. To determine the 2nd-order critical lines, we employed a standard finite-size scaling analysis of the specific heat C_v, for linear system sizes $N = 24,\ 36,\ 48$, and 60 (ie., for $3N^3$ spins). First-order critical points were identified and located using energy distributions. These distributions are bi-modal (have two maxima) for the first-order transitions and single-modal otherwise. We thermalized our samples for up to 10^6 MC sweeps (one sweep having $3N^3$ elementary updates). The data were accumulated for $\sim 4 \times 10^8$ MC sweeps.

The resulting phase diagram is presented in Fig.1. The first-order transition coinciding with the self-duality line was observed for $0.2575(5) > \lambda_{\rm bond} > 0.22635(5)$. Outside of this interval we saw no bi-modal structure in the energy distribution for system sizes up to $N = 60$. The inset of Fig.2 shows the evolution of the energy distribution function along the self-dual line. Even when the bi-modal structure is observed it is extremely weak, developing only for large N, and the distribution can be sampled in the minimum without flat-histogram or similar reweighting techniques.

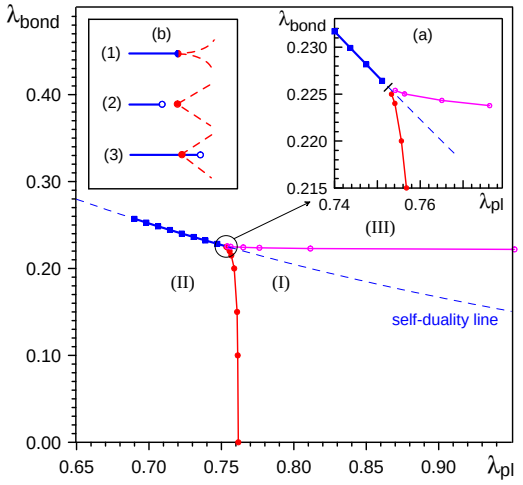

FIG. 1: (color online). The phase diagram of the Hamiltonian (9). Circles correspond to the second-order transitions (open and filled symbols are related by the duality transformation). Filled squares describe the first-order self-dual transitions. Bold and dashed lines are used to guide an eye and correspond to the 1st- and 2nd-order transitions, respectively. The phases are: (I) - topological phase; (II) - topologically disordered phase; (III) - magnetically ordered phase. In inset (a) we show the region where all phases meet each other. In inset (b) we show three alternative ways of connecting the lines.

As noted above, these results conflict with previous MC simulations in Ref. [10], who suggest the 1st-order line splits into two 1st-order lines. The inset (a) of Fig.1 shows a closeup of the controversial region. Though we were able to resolve critical points with an accuracy of at least three digits, we observed no splitting of the self-dual 1st-order line into two 1st-order transitions. We also find no evidence for tri-critical points on the Ising-type lines as long as we can resolve two separate transitions. There remains a tiny parameter range between the apparent disappearance of the bi-modal distribution on the self-dual line (this disappearance probably due to our limited system size) and two resolved 2nd-order transitions.

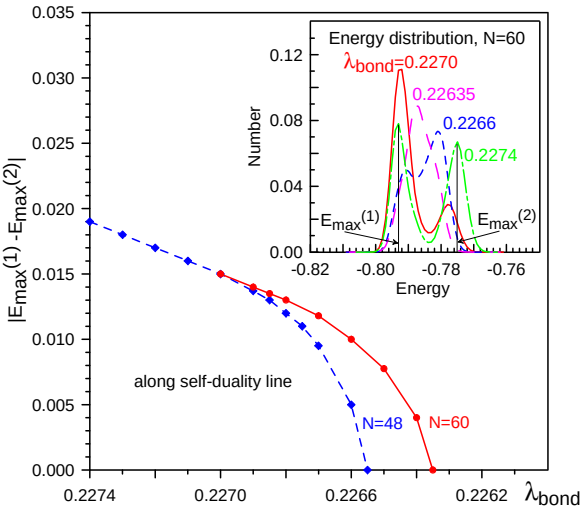

FIG. 2: (color online). The distance between two maxima in bi-modal energy distributions along the self-duality line for $N = 60$ as a function of $\lambda_{\rm bond}$. The inset shows examples of the energy distributions at various values of $\lambda_{\rm bond}$.

To probe the behavior in this tiny parameter range we need a different approach. We therefore scanned energy distributions at 30 points ($N = 48$) along the line perpendicular to the self-duality line right in the questionable region (short solid line in the inset (a)). If the 1st-order line were to split above the scan, the third maximum would have to emerge in the energy distribution right between the two maxima we observe on the self-dual line - implying that the energy maxima on the self-dual line could not merge smoothly, and right below the split, three maxima would have to be seen in the energy distribution. However all distributions along the scan were found to have only one peak. It is also clear from the main part of Fig.2 that on the self-duality line, the energy maxima approach each other and merge continuously as $\lambda_{\rm bond}$ increases. The curves presented in Fig.2 follow a power law near the vanishing point, with corresponding critical exponent ~ 0.55.

We thus conclude that the split 1st-order scenario does not work. Instead there are three possibilities. Either all three lines merge at one point (case (1) in the inset (b), Fig.1); or the 1st-order line ends *before* or *after* the point where two 2nd-order lines touch the self-dual

line (cases (2) and (3) in the inset (b), Fig.1). Unfortunately our data cannot distinguish between the alternatives because the 2nd-order lines seem to touch at extremely small (possibly zero) angle. Formally, option (2) fits the data best. Theoretically, the last two scenarios are less demanding since they fit the existing theory of phase transitions (our data suggest that the 2nd-order transitions cannot merge into a single smooth curve and form a kink at the self-dual line). We are not aware of any effective theory leading to the first scenario.

Phases. Using the two correspondence equations

$$\tilde{h}_z = -\frac{1}{2}\ln\tanh(\tilde{J}_x) = \lambda_{\rm bond}; \qquad (10a)$$

$$\tilde{J}_z = -\frac{1}{2}\ln\tanh(\tilde{h}_x) = \lambda_{\rm pl}, \qquad (10b)$$

we can reformulate the phase diagram Fig.1 in terms of the renormalized parameters $\tilde{J}_x$, $\tilde{J}_z$, $\tilde{h}_x$ and $\tilde{h}_z$ of the TCM. The resulting phase diagram in terms of the external fields is presented in Fig.3. Let us go through the phases in this Figure.

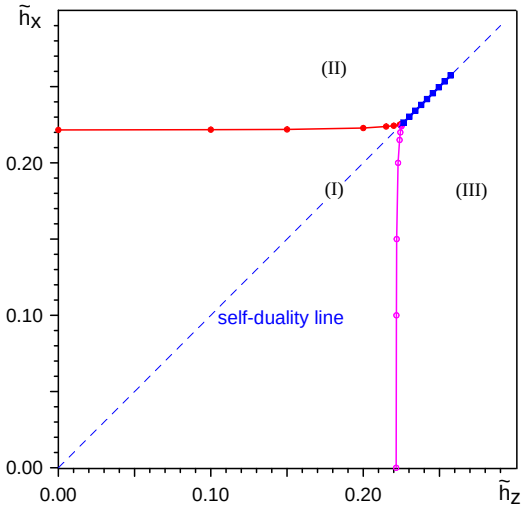

FIG. 3: (color online). The phase diagram Fig.1 in terms of the renormalized external fields, $\tilde{h}_x = h_x\Delta\tau$ and $\tilde{h}_z = h_z\Delta\tau$, of the model (2). The phases (I), (II) and (II) are the same as in Fig.1.

The phase (I) corresponds to the topological phase of the model (2) (the "free charge" phase of the isotropic $\mathbb{Z}_2$ Higgs model (HM), [9]). In this phase the system tends to have all $B_p = 1$ and $A_s = 1$ and a realization of such a state is obviously not unique. The plaquettes with $B_p = -1$ (magnetic vortices) and vertices with $A_s = -1$ (electric charges) appear mainly in the vicinity of the critical lines between the phases (I) and (II) (vortices) and (I) and (III) (charges). The phase (III) may be called "magnetically ordered" since the spins are mostly polarized in the z-direction. However, $\langle\sigma^z\rangle$ also has nonzero value everywhere in the phase diagram. The true order parameter may be written as $\langle\mu^z\rangle$ using the gauge-symmetrized Hamiltonian (4). A non-zero value of this parameter results in the confinement of magnetic vortices (no free vortices) and the condensation of electric charges. In the HM this is the "Higgs" phase. The phase (II) is characterized by a dual order parameter related to $\langle\sigma^x\rangle$, which can be defined by rewriting the Hamiltonian in different variables. Its nonzero value results in non-conservation of total magnetic "charge" and condensation of magnetic vortices while electric charges are confined (no free charges). This phase corresponds to the "confinement" phase of the HM. The transition between the phases (II) and (III) is accompanied by a sharp change in the number of vortices and charges, corresponding to a "liquid-gas" type transition. The self-duality symmetry reflects the symmetry between charges and vortices.

Summary. The topological phase of the toric code model (the "free charge" phase of the 3d gauge Higgs model) remains stable in a rather wide range of fields and breaks down via two Ising type transitions whose critical lines meet with the 1st-order one corresponding to a liquid-gas type transition. The 1st-order line either meets with two 2nd-order lines in one multicritical point, or terminates before or after the point where two 2nd-order lines touch the self-duality line. The construction of an effective field theory for this multicritical region is an interesting open problem.

We thank E. Fradkin, B. Svistunov, S. Trebst, M. Troyer, I. Affleck, and K. Shtengel for discussions. We are also indebted to M. Berciu and J. Heyl whose research clusters were used to perform our MC simulations.

[1] P.W.Anderson, *Science* **235**, 1196, (1987).
[2] N. Read, B. Chakraborty, Phys. Rev. B **40**, 7133 (1989).
[3] A.Yu. Kitaev, Ann. Phys. (N.Y.) 303, 2 (2003).
[4] G. Misguich, D. Serban, V. Pasquier, Phys. Rev. Lett. **89**, 137202 (2002); `cond-mat/0204428`.
[5] N. Read, S. Sachdev, Phys. Rev. Lett. **66**, 1773 (1991).
[6] R. Moessner, S. L. Sondhi, Phys. Rev. Lett. **86**, 1881 (2001); `cond-mat/0007378`.
[7] S. Trebst, P. Werner, M. Troyer, K. Shtengel, and Ch. Nayak, PRL **98**, 070602 (2007).
[8] F.J. Wegner, J. of Math. Phys. **12**, 2259 (1971).
[9] E. Fradkin and S. Shenker, Phys. Rev. D **19**, 3682 (1979).
[10] G.A. Jongeward, J.D. Stack and C. Jayaprakash, Phys. Rev. D **21**, 3360 (1980).
[11] M. Suzuki, Progress on Theor. Phys. **56**, 1454 (1976).
[12] R. Gupta and P. Tamayo, *The critical exponents for the 3d Ising model*, US-Japan Bilateral Seminar - Maui, August 28-31, 1996.
[13] R. Balian, J.M. Drouffe, and C. Itzykson, Phys. Rev. D **11**, 2098 (1975).